Structure of the Pairing Interaction in the Two-Dimensional Hubbard Model

T. A. Maier,[1,*] M. S. Jarrell,[2,†] and D. J. Scalapino[3,‡]

[1]Computer Science and Mathematics Division, Oak Ridge National Laboratory, Oak Ridge, Tennessee 37831-6164, USA
[2]Department of Physics, University of Cincinnati, Cincinnati, Ohio 45221, USA
[3]Department of Physics, University of California, Santa Barbara, California 93106-9530, USA

(Received 15 August 2005; published 2 February 2006)

Dynamic cluster Monte Carlo calculations for the doped two-dimensional Hubbard model are used to study the irreducible particle-particle vertex responsible for $d_{x^2-y^2}$ pairing in this model. This vertex increases with increasing momentum transfer and decreases when the energy transfer exceeds a scale associated with the $Q = (\pi, \pi)$ spin susceptibility. Using an exact decomposition of this vertex into a fully irreducible two-fermion vertex and charge and magnetic exchange channels, the dominant part of the effective pairing interaction is found to come from the magnetic, spin $S = 1$ exchange channel.

DOI: 10.1103/PhysRevLett.96.047005 PACS numbers: 74.20.−z, 71.10.−w, 71.27.+a, 74.72.−h

Numerical studies of the doped two-dimensional Hubbard model have shown that strong $d_{x^2-y^2}$ pairing correlations develop as the temperature is lowered [1] and recent work has provided evidence that the Hubbard model near half filling does have a superconducting ground state [2–4]. In spite of this progress, the goal of using numerical methods to determine the nature of the pairing mechanism has proven elusive. In this Letter we develop a new approach which combines numerical and diagrammatic methods to determine the structure of the pairing interaction in the doped two-dimensional Hubbard model. Our study will focus on the 4-point vertex shown in Fig. 1, calculated with a quantum Monte Carlo dynamic cluster approximation (QMC-DCA) [5–7]. From this vertex and the QMC-DCA results for the single-particle Green's function, we have determined the irreducible particle-particle and particle-hole vertices. The leading low temperature eigenvalue of the Bethe-Salpeter equation for the particle-particle channel is shown to have $d_{x^2-y^2}$ symmetry. We then examine the momentum and energy dependence of the irreducible particle-particle vertex. Decomposing this vertex into the sum of a fully irreducible two-fermion vertex and particle-hole exchange magnetic ($S = 1$) and charge density ($S = 0$) channels, we find that the dominant contribution to the pairing interaction comes from the magnetic ($S = 1$) exchange.

The Hubbard model that we study has a near-neighbor, one-electron hopping t and an on-site Coulomb interaction U:

$$H = -t\sum_{\langle ij\rangle\sigma}(c^\dagger_{i\sigma}c_{j\sigma} + c^\dagger_{j\sigma}c_{i\sigma}) + U\sum_i n_{i\uparrow}n_{i\downarrow} - \mu\sum_{i\sigma}c^\dagger_{i\sigma}c_{i\sigma}. \tag{1}$$

We will take $U/t = 4$ and adjust μ so that the average site occupancy $\langle n_i\rangle = 0.85$. We have carried out dynamical cluster Monte Carlo calculations [5–7] for the 24-site k cluster shown in the inset of Fig. 2.

For a 2D system the dynamical cluster approximation maps the original lattice model onto a periodic cluster of size $N_c = L_c^2$ embedded in a self-consistent host [5–7]. The essential assumption is that short-range quantities, such as the self energy and its functional derivatives (the irreducible vertex functions) are well represented as diagrams constructed from the coarse-grained Green's function. To this end, the first Brillouin zone is divided into N_c cells, with each cell represented by its center wave vector $\mathbf{K}$ surrounded by N/N_c lattice wave vectors labeled by $\tilde{\mathbf{k}}$. The reduction of the N-site lattice problem to an effective N_c-site cluster problem is achieved by coarse graining the single-particle Green's function, i.e., averaging $G(\mathbf{K} + \tilde{\mathbf{k}})$ over the $\tilde{\mathbf{k}}$ within a cell which converges to a cluster Green's function $G_c(\mathbf{K})$. Consequently, the compact Feynman diagrams constructed from $G_c(\mathbf{K})$ collapse onto those of an effective cluster problem embedded in a host which accounts for the fluctuations arising from the hopping of electrons between the cluster and the rest of the system. The compact cluster quantities are then used to calculate the corresponding lattice quantities.

For example, the DCA cluster one- and two-particle Green's functions that we calculate have the standard finite temperature definitions

$$G_{c\sigma}(X_2, X_1) = -\langle T_\tau c_\sigma(X_2)c^\dagger_\sigma(X_1)\rangle \tag{2a}$$

$$G_{c2\sigma_4\cdots\sigma_1}(X_4, X_3; X_2, X_1) = -\langle T_\tau c_{\sigma_4}(X_4)c_{\sigma_3}(X_3) \times c^\dagger_{\sigma_2}(X_2)c^\dagger_{\sigma_1}(X_1)\rangle. \tag{2b}$$

Here, $X_\ell = (\mathbf{X}_\ell, \tau_\ell)$, where $\mathbf{X}_\ell$ denotes a site in the DCA cluster, τ_ℓ is the imaginary time, T_τ is the usual τ-ordering operator, and $c^{(\dagger)}_\sigma(X_2)$ destroys (creates) a particle on the cluster with spin σ. Fourier transforming on both the cluster space and imaginary time variables gives $G_c(K)$ and $G_{c2}(K_4, K_3; K_2, K_1)$ with $K = (\mathbf{K}, i\omega_n, \sigma)$. Using $G_c(K)$ and $G_{c2}(K_4, K_3; K_2, K_1)$, one can extract the cluster four-point vertex Γ from

$$G_{c2}(K_4,K_3;K_2,K_1) = -G_c(K_1)G_c(K_2) \times [\delta_{K_1,K_4}\delta_{K_2,K_3} - \delta_{K_1,K_3}\delta_{K_2,K_4}] + \frac{T}{N}\delta_{K_1+K_2,K_3+K_4}G_c(K_4)G_c(K_3) \times \Gamma(K_4,K_3;K_2,K_1) \times G_c(K_2)G_c(K_1). \quad (3)$$

Then, using G_c and Γ, one can determine the irreducible particle-particle and particle-hole vertices Γ^{pp} and Γ^{ph} from the Bethe-Salpeter equations shown in Figs. 1(a) and 1(b). There is a second particle-hole vertex but it is simply related to Γ^{ph}. Note that Γ^{ph} and Γ^{pp} do not have a subscript c, since both the lattice and the cluster share these compact quantities. Because of the rotational invariance of the Hubbard model, it is convenient to separate the particle-particle channels into singlet and triplet and the particle-hole channels into a magnetic part which carries spin $S = 1$ and a charge density part which has $S = 0$.

In order to determine the nature of the low temperature correlations, we use these irreducible vertices and the lattice single-particle Green's function to calculate the Bethe-Salpeter eigenvalues and eigenfunctions in various channels. For example, in the particle-particle channel

$$-\frac{T}{N}\sum_{k'}\Gamma^{pp}(K,-K;K',-K')G_\uparrow(k')G_\downarrow(-k')\phi_\alpha(K') = \lambda_\alpha\phi_\alpha(K) \quad (4)$$

with a similar equation using Γ^{ph} for the particle-hole channel. Here, the sum over k' denotes a sum over both momentum $\mathbf{k}'$ and Matsubara $\omega_{n'}$ variables. We decompose $\mathbf{k}' = \mathbf{K}' + \tilde{\mathbf{k}}'$. By assumption, irreducible quantities like Γ^{pp} and ϕ_α do not depend on $\tilde{\mathbf{k}}'$, allowing us to coarse-grain the Green function legs, yielding an equation that depends only on coarse-grained and cluster quantities

$$-\frac{T}{N_c}\sum_{K'}\Gamma^{pp}(K,-K;K',-K')\bar{\chi}_0^{pp}(K')\phi_\alpha(K') = \lambda_\alpha\phi_\alpha(K) \quad (5)$$

with $\bar{\chi}_0^{pp}(K') = \frac{N_c}{N}\sum_{\tilde{\mathbf{k}}'}G_\uparrow(\mathbf{K}'+\tilde{\mathbf{k}}', i\omega_{n'})G_\downarrow(-\mathbf{K}'-\tilde{\mathbf{k}}', -i\omega_{n'})$.

In Fig. 2 we show the leading eigenvalue versus temperature for the pairing, charge density, and magnetic channels for $U/t = 4$ and $\langle n\rangle = 0.85$. As the temperature is reduced, the leading particle-hole eigenvalue occurs in the magnetic channel and has a center of mass momentum $\mathbf{Q} = (\pi,\pi)$ and $\omega_m = 0$. Previous Monte Carlo calculations on 8×8 lattices show that for this doping the peak response is slightly shifted from (π,π), but our 24-site cluster lacks the resolution to see this [8]. This antiferromagnetic eigenvalue grows and then saturates at low temperatures. The leading particle-particle eigenvalue is a spin singlet and, as shown in the inset of Fig. 3, its eigenfunction $\phi_{d_{x^2-y^2}}$ has $d_{x^2-y^2}$ symmetry. The ω_n frequency dependence of the normalized gap function $\phi_{d_{x^2-y^2}}(\mathbf{K},\omega_n)$ at the antinodal point $\mathbf{K} = (\pi,0)$ is plotted in Fig. 3. As shown, it is even in ω_n, corresponding to a $d_{x^2-y^2}$-wave singlet, even frequency pairing. Also plotted in this figure

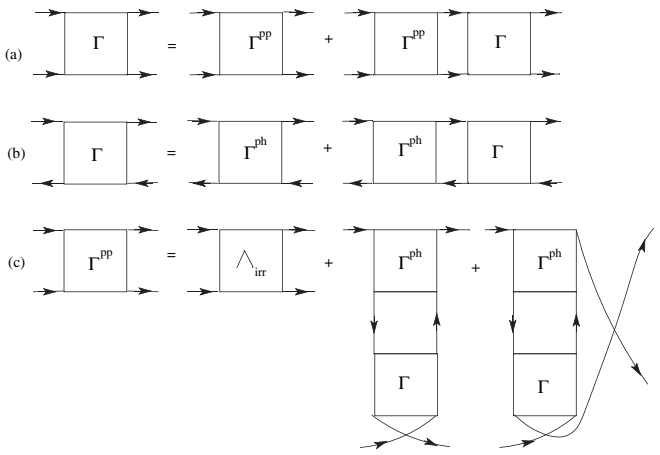

FIG. 1. Bethe-Salpeter equations for (a) the particle-particle and (b) the particle-hole channels showing the relationship between the full vertex, the particle-particle irreducible vertex Γ^{pp}, and the particle-hole irreducible vertex Γ^{ph}, respectively. (c) Decomposition of the irreducible particle-particle vertex Γ^{pp} into a fully irreducible two-fermion vertex Λ_{irr} plus contributions from the particle-hole channels. All diagrams represent DCA cluster quantities, including the Green function legs.

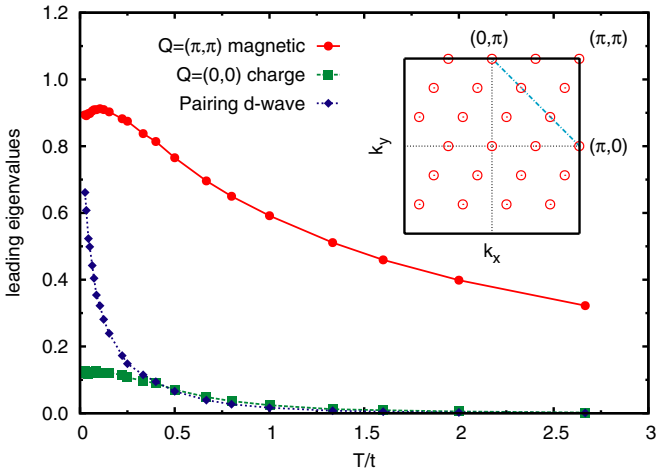

FIG. 2 (color online). Leading eigenvalues of the Bethe-Salpeter equation [e.g., Eq. (5)] in various channels for $U/t = 4$ and a site occupation $\langle n\rangle = 0.85$. The $\mathbf{Q} = (\pi,\pi)$, $\omega_m = 0$, $S = 1$ magnetic eigenvalue is seen to saturate at low temperatures. The leading eigenvalue in the singlet $\mathbf{Q} = (0,0)$, $\omega_m = 0$ particle-particle channel has $d_{x^2-y^2}$ symmetry and increases toward 1 at low temperatures [2]. The largest charge density eigenvalue occurs in the $\mathbf{Q} = (0,0)$, $\omega_m = 0$ channel and saturates at a small value. The inset shows the distribution of k points for the 24-site cluster we have studied.

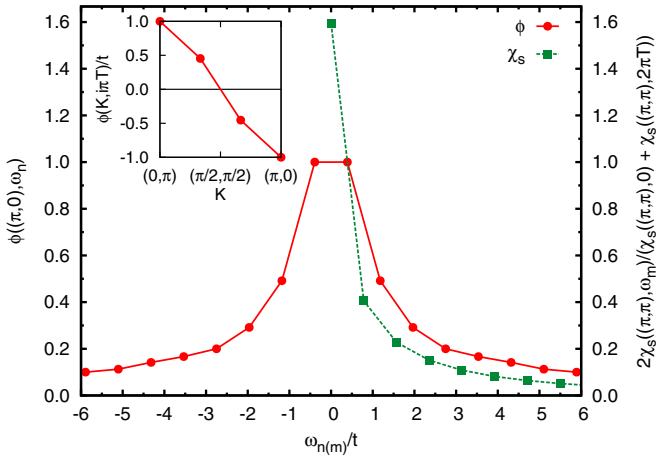

FIG. 3 (color online). The Matsubara frequency dependence of the eigenfunction $\phi_{d_{x^2-y^2}}(\mathbf{K}, \omega_n)$ of the leading particle-particle eigenvalue of Fig. 2 for $\mathbf{K} = (\pi, 0)$ normalized to $\phi(\mathbf{K}, \pi T)$ (solid line, red online). Here, $\omega_n = (2n + 1)\pi T$ with $T = 0.125t$. The Matsubara frequency dependence of the normalized magnetic spin susceptibility $2\chi(\mathbf{Q}, \omega_m)/[\chi(\mathbf{Q}, 0) + \chi(\mathbf{Q}, 2\pi T)]$ for $\mathbf{Q} = (\pi, \pi)$ versus $\omega_m = 2m\pi T$ (dashed line, green online). Inset: The momentum dependence of the eigenfunction $\phi_{d_{x^2-y^2}}(\mathbf{K}, \pi T)$ normalized to $\phi_{d_{x^2-y^2}}((0, \pi), \pi T)$ shows its $d_{x^2-y^2}$ symmetry. Here, $\omega_n = \pi T$ and the momentum values correspond to values of $\mathbf{K}$ which lay along the dashed line shown in the inset of Fig. 2.

is the ω_m dependence of the $\mathbf{Q} = (\pi, \pi)$ spin susceptibility $\chi(\mathbf{Q}, \omega_m)$ normalized to coincide with $\phi_{d_{x^2-y^2}}(\mathbf{K}, \omega_n)$ at $\omega_n = \pi T$. The Matsubara frequency which enters the gap function corresponds to a fermion frequency $\omega_n = (2n + 1)\pi T$, while $\omega_m = 2m\pi T$ for the spin susceptibility, leading to the interlacing of points shown in Fig. 3. From the momentum and frequency dependence of the gap function $\phi(\mathbf{K}, \omega_n)$, it follows that the irreducible particle-particle vertex is an increasing function of the momentum transfer and is characterized by the same energy scale that enters the spin susceptibility $\chi(\mathbf{Q}, \omega_m)$. At larger values of U it will be interesting to see if there is an increased tendency for a finite response at large Matsubara frequencies indicating a contribution from the upper Hubbard band.

To learn more about the mechanism responsible for $d_{x^2-y^2}$ pairing in the doped Hubbard model, it is useful to decompose the pairing interaction Γ^{pp} as shown in Fig. 1(c). Here, the irreducible particle-particle vertex is given as a combination of a fully irreducible two-fermion vertex $\wedge_{irr}$ and partially reducible particle-hole exchange contributions [9,10]. For the even frequency, even momentum part of the irreducible particle-particle vertex $\Gamma^{pp}_{even}(K, K') = 1/2[\Gamma^{pp}(K, K') + \Gamma^{pp}(K, -K')]$, we obtain

$$\Gamma^{pp}_{even}(K, K') = \wedge_{irr}(K, K') + \tfrac{1}{2}\Phi_d(K, K') + \tfrac{3}{2}\Phi_m(K, K') \tag{6}$$

with $K = (\mathbf{K}, i\omega_n)$. The subscripts d and m denote the charge density ($S = 0$) and magnetic ($S = 1$) particle-hole channels

$$\begin{aligned}\Phi_{d/m}(K, K') = \tfrac{1}{2}[&\Gamma_{d/m}(K - K'; K', -K) \\ &- \Gamma^{ph}_{d/m}(K - K'; K', -K) \\ &+ \Gamma_{d/m}(K + K'; -K', -K) \\ &- \Gamma^{ph}_{d/m}(K + K'; -K', -K)].\end{aligned} \tag{7}$$

On the right hand side, the first label is for the center of mass, and the second and third for the relative wave vectors and frequencies. Using the Monte Carlo results for G and Γ, we have solved the t-matrix equations shown in Figs. 1(a) and 1(b) to determine Γ^{pp}, Φ_d and Φ_m. Then, substituting these into Eq. (6), we have determined the fully irreducible vertex $\wedge_{irr}$.

Monte Carlo results for the irreducible particle-particle vertex Γ^{pp} obtained from the 24-site cluster approximation are shown in Fig. 4(a). Here, we set $\omega_n = \omega'_n = \pi T$, $\mathbf{K} = (\pi, 0)$ and $\mathbf{K}'$ takes momentum values along the dashed line shown in the inset of Fig. 2. As the temperature is lowered, Γ^{pp} increases as the momentum transfer $\mathbf{q} = \mathbf{K} - \mathbf{K}'$ increases as one expects for a d-wave pairing interaction. To understand the origin of this behavior, the contributions of the particle-hole ($S = 0$) charge density and ($S = 1$) magnetic channels are plotted in Figs. 4(c) and 4(d) respectively and the contribution from the fully irreducible vertex $\wedge_{irr}$ is shown in Fig. 4(b). It is clear that the dominant contribution to Γ^{pp} comes from the $S = 1$ magnetic channel. The charge density channel and the fully irreducible vertex are basically flat in momentum and change relatively little as the temperature is reduced. Thus, based upon the decomposition of the irreducible particle-particle interaction shown in Fig. 4, we conclude that the pairing mechanism in the doped two-dimensional Hubbard model is mediated by the exchange of $S = 1$ particle-hole spin-fluctuations.

To summarize, we have studied the pairing interaction Γ^{pp} of a doped $\langle n \rangle = 0.85$, two-dimensional Hubbard model with $U/t = 4$. We found that the eigenfunction $\phi(\mathbf{K}, i\omega_n)$ of the leading low temperature eigenvalue in the particle-particle pairing channel is an even frequency singlet with $d_{x^2-y^2}$ symmetry. The momentum and frequency dependence of $\phi(\mathbf{K}, i\omega_n)$ imply that Γ^{pp} increases as the momentum transfer $\mathbf{q} = \mathbf{K} - \mathbf{K}'$ increases and that its dynamics is set by the same characteristic energy scale as the spin susceptibility. It was also found to increase as the temperature was lowered, saturating when the leading antiferromagnetic eigenvalue stopped growing. Finally, using an exact decomposition of Γ^{pp}, we showed that the dominant contribution to this interaction comes from the $S = 1$ particle-hole channel. We believe that the calculation and analysis of the four-point vertex provides a useful, unbiased method for determining the nature of the leading

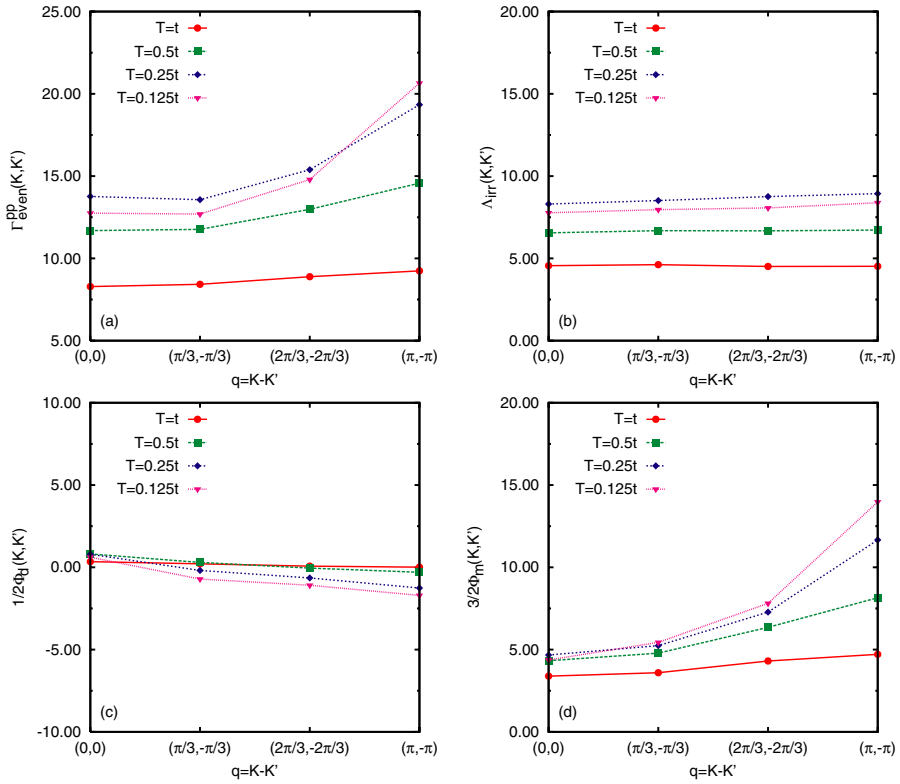

FIG. 4 (color online). (a) The irreducible particle-particle vertex Γ^{pp} versus $\mathbf{q} = \mathbf{K} - \mathbf{K}'$ for various temperatures with $\omega_n = \omega_{n'} = \pi T$. Here, $\mathbf{K} = (\pi, 0)$ and $\mathbf{K}'$ moves along the momentum values of the 24-site cluster which lay on the dashed line shown in the inset of Fig. 2. Note that the interaction increases with the momentum transfer as expected for a d-wave pairing interaction. (b) The $\mathbf{q}$ dependence of the fully irreducible two-fermion vertex $\wedge_{irr}$. (c) The $\mathbf{q}$ dependence of the charge density ($S = 0$) channel $\frac{1}{2}\Phi_d$ for the same set of temperatures. (d) The $\mathbf{q}$ dependence of the magnetic ($S = 0$) channel $\frac{3}{2}\Phi_m$.

correlations of interacting many-electron systems and the structure of the mechanisms responsible for them.

We acknowledge useful discussions with W. Putikka, R. Sugar, and S.-C. Zhang. This research was enabled by computational resources of the Center for Computational Sciences and in part supported by the Laboratory Research and Development program at Oak Ridge National Laboratory. Part of this research was conducted at the Center for Nanophase Materials Sciences, which is funded by the Division of Scientific User Facilities, U.S. Department of Energy. This research was supported by NSF Grants No. DMR-0312680 and No. DMR02-11166.

*Electronic address: maierta@ornl.gov
†Electronic address: jarrell@physics.uc.edu
‡Electronic address: djs@vulcan2.physics.ucsb.edu

[1] N. Bulut, D. J. Scalapino, and, S. R. White, Phys. Rev. B **47**, R6157 (1993); **47**, 14 599 (1993).
[2] T. A. Maier, M. Jarrell, T. C. Schulthess, P. R. C. Kent, and J. B. White, Phys. Rev. Lett. **95**, 237001 (2005).
[3] David Sénéchal, P.-L. Lavertu, M.-A. Marois, and A.-M. S. Tremblay, Phys. Rev. Lett. **94**, 156404 (2005).
[4] S. S. Kancharla, M. Civelli, M. Capone, B. Kyung, D. Sénéchal, G. Kotliar, and A.-M. S. Tremblay, cond-mat/0508205.
[5] M. Jarrell, T. Maier, C. Huscroft, and S. Moukouri, Phys. Rev. B **64**, 195130 (2001).
[6] M. H. Hettler, A. N. Tahvildar-Zadeh, M. Jarrell, T. Pruschke, and H. R. Krishnamurthy, Phys. Rev. B **58**, R7475 (1998); M. H. Hettler, M. Mukherjee, M. Jarrell, and H. R. Krishnamurthy, *ibid.* **61**, 12 739 (2000).
[7] Th. Maier *et al.*, Rev. Mod. Phys. **77**, 1027 (2005).
[8] A. Moreo, D. J. Scalapino, R. L. Sugar, S. R. White, and N. E. Bickers, Phys. Rev. B **41**, 2313 (1990).
[9] M. Pfitzner and P. Wölfle, Phys. Rev. B **35**, 4699 (1987).
[10] G. Esirgen and N. E. Bickers, Phys. Rev. B **57**, 5376 (1998).